ELSEVIER

Thin Solid Films 333 (1998) 196–202

thin solid films

Electrical and optical properties of fluorine-doped ZnO thin films prepared by spray pyrolysis

A. Sanchez-Juarez[a,*], A. Tiburcio-Silver[b], A. Ortiz[c], E.P. Zironi[d], J. Rickards[d]

[a]*Departamento de Materiales Solares, Centro de Investigación en Energía, UNAM, Apto. Postal 34, Temixco, Morelos, 62580 Mexico*
[b]*Div. de Estudios de Posgrado, Instituto Tecnológico de Toluca, SEP, Mexico*
[c]*Instituto de Investigaciones en Materiales, Apdo. Postal 70-360, Mexico D.F. 04510, Mexico*
[d]*Instituto de Física, UNAM, Apdo. Postal 20-364, Mexico D.F. 01000, Mexixo*

Received 29 October 1997; accepted 24 April 1998

Abstract

Undoped and fluorine-doped ZnO thin films deposited by spray pyrolysis onto soda-lime glass substrates were electrically and optically characterized. Resistivities as low as 1×10^{-1} Ω cm, Hall mobility as high as 10 cm^2/V per s and effective carrier concentration as high as 4×10^{19} cm^{-3} have been obtained. Relative fluorine concentration was determined by the resonant nuclear reaction method. Electron concentrations due to the fluorine incorporation as an effective electrically active donor is always lower than fluorine contents on the films and in the starting solution. Average optical transmisttance on the whole visible range as high as 92% (substrate losses not included) have been obtained for the best conductive films. The refractive index of layers was found to increase with fluorine doping and substrate temperature. The fluorine incorporation, at ZnO thin films, results in a band gap widening effect.

Keywords: Nuclear reaction; Optical properties; X-ray diffraction; Zinc oxide

1. Introduction

Due to their optical and electrical properties metal oxide semiconductor films have been widely studied and have received considerable attention in recent years. Some of them are good candidates for transparent conductive films, if they are prepared off-stoichiometry or doped with suitable impurities. Such films have applications in electronic and optoelectronic devices, photothermal and photovoltaic conversion, etc. ZnO is one of the metal oxide semiconductors suitable for use in optoelectronic devices, as an alternative material to tin oxide and indium tin oxide. Pure zinc oxide is an intrinsic semiconductor with high electrical resistivity and a direct band gap of about 3.2 eV at 298 K [1,2]. Hence, in the form of thin film, the material can be made transparent in the whole visible range. The first applications of zinc oxide compound has been in chemical and pharmaceutical applications. ZnO is a non-ferroelectric compound and it has a large enough electromechanical coupling coefficient. Due to this fact, ZnO is a well known piezoelectric material which has been used as a transducer for surface acoustic wave devices (SAW) [3] and delay line [4] devices. The emergence on zinc oxide thin films in the last two decades as a transparent conductor oxide for photovoltaic applications and as a gas sensor device [5,6], has generated a renewed interest in their optical and electrical properties.

ZnO thin films have been prepared by a variety of thin films deposition techniques, such as vacuum thermal evaporation [7], reactive DC and RF magnetron sputtering [8–11], chemical vapor deposition [12–15], dip-coating method [16,17], electrochemical deposition [18], reactive thermal evaporation [19], pneumatic spray pyrolysis technique [20–24], ultrasonic spray pyrolysis [25,26], charged liquid cluster beam [27], etc. It was found that the optoelectronical properties of ZnO thin films depend strongly on the deposition processes.

ZnO is an n-type semiconductor, its electrical conductivity is mainly due to zinc excess at interstitial position [28]. Its electric properties could be modified thoroughly by thermal treatment with hydrogen [29], or by an appropriate doping process, either by cationic [20,21,25] or anionic [15,30,31] substitution. The electrical conductivity of ZnO thin films can increase by cationic substitution with positive trivalent atoms. By using positive monovalent atoms, a

* Corresponding author. Fax: +52 73 25 00 18; e-mail: asj@mazatl.cie.unam.mx.

0040-6090/98/$ - see front matter
PII S0040-6090(98)00851-7

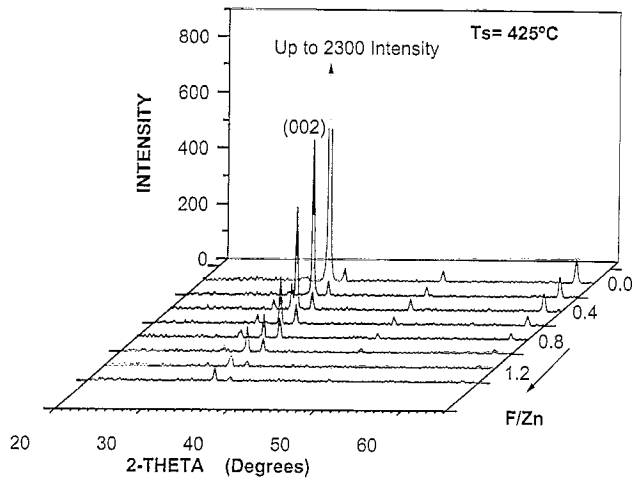

Fig. 1. X-ray diffractograms of ZnO:F thin films grown at 425°C substrate temperature at different F/Zn atomic ratios in the starting solution.

decrease in the electrical conductivity results. On the other hand, anionic substitution with negative monovalent atoms leads to an increase in the electrical conductivity. Wherever the impurity is incorporated, the anionic or cationic substitution affects the optical properties of these materials [21,32].

In a previous paper [31] we reported on the general properties of fluorine-doped ZnO thin films deposited onto Pyrex glass by spray pyrolysis. There, we presented and analyzed the dependence of the properties of these films on the growth and the crystal structure. In this paper we shall deal with a detailed analysis of the electrical and optical properties of the spray pyrolytically deposited fluorine doped ZnO thin films.

2. Experimental

The preparation of undoped and fluorine-doped ZnO thin films by spray pyrolysis has already been described [31]. The films were deposited onto soda-lime glass slices and single crystal Si of 1.5×2.5 cm, chemically and ultrasonically cleaned. A 0.05 M solution of zinc acetate dehydrated dissolved in a mixture of three parts of methanol and one part in volume of deionized water was used. The substrate temperature (T_s) was varied from 300 to 500°C in 25°C steps. Fluorine doping was achieved by adding ammonium fluoride to the starting solution. The doping level in the solution, designated by F/Zn atomic ratio, was varied from 0.0 to 1.0 in 0.1 steps. The thickness of the film was measured by means of a profilometer Alpha Step model 100 from Tencor Instruments. The required step was made during the deposition of the film by blocking part of the substrate by a thin coverglass. The measured thickness was confirmed by an ellipsometric technique. The optical and electrical characterizations were made on films having 200 ± 25 nm in thickness. Electrical contacts to the films were made with four indium strips deposited by vacuum thermal evaporation. The lateral electrical conductivity measurements of the films were automatically carried out by the four-point probe method. Resistivity, Hall mobility and effective carrier concentration, have been calculated from Hall–Van der Pauw measurements.

The optical transmittance at normal incidence and specular reflectance of the films, were measured with a double-beam spectrophotometer Shimadzu model 3101PC in the UV-vis-NIR region (300–2500 nm). All optical measurements were performed having air as the reference. The average optical transmittance in the visible region for a naked clean substrate was 91%. From these data, and using an analytic technique developed by Manifacier et al. [33], we have calculated the film thickness and the evolution of their refraction index (n) in the whole explored range. The optical band gap (E_g) of the films has been calculated from the dependence of the absorption coefficient (α) on the photon energy ($h\nu$) taking into account that ZnO is a direct band gap semiconductor [1,2]. All the electrical and optical measurements were carried out at room temperature.

The structural properties were studied by X-ray diffraction measurements (Siemens D-500) using the CuKα radiation with $\lambda = 1.5405$ Å. The average dimension of crystallites was determined by the Scherrer method from the broadening of the diffraction peaks taking into account the instrumental broadening.

In order to understand the influence of the fluorine incorporated at ZnO thin films on the physical properties, we applied the resonant nuclear reaction (RNR) technique to determine the fluorine content and its distribution in the film. For this experiment ZnO:F thin films with a thickness of 90 nm were used. RNR technique has shown to be a sensitive probe when applied to fluorine doped tin oxide thin films [34,35]. It consists of bombarding the sample with protons having an energy in the vicinity of an isolated resonance in a reaction with fluorine. We used the proton beam from the 700 keV Van de Graaff accelerator of Instituto de Física, UNAM, to excite the $^{19}F(p,\alpha\gamma)^{16}O$ nuclear reaction, in the vicinity of the well known, high cross section, 2.4 keV wide resonance at a proton energy of 340 keV. Since the resonance energy is characteristic of this particular reaction, and no competition reactions with zinc, oxygen. or other possible contaminants appear in the energy interval covered, there is no doubt as to the identification of fluorine. The 6.14 MeV γ-rays and two escape peaks from the reaction were detected in either a 10.2×10.2 cm or a 5.1×5.1 cm NaI(Tl) scintillation detector. A schematic diagram of the experimental set-up was reported elsewhere [35].

3. Results and discussions

In our previous paper [31] we have reported on the structural properties and its correlation with the general proper-

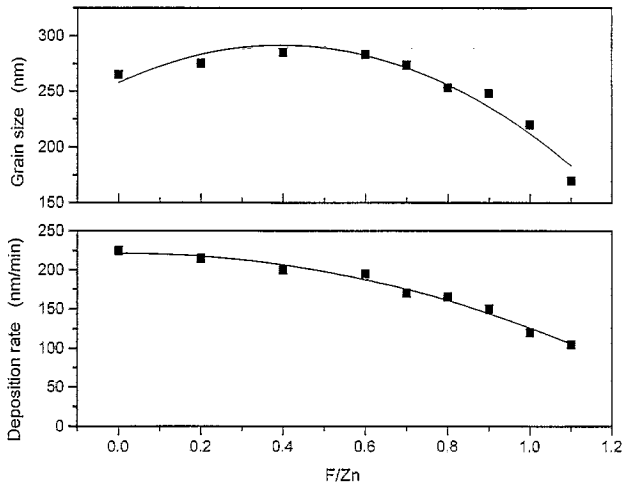

Fig. 2. Dependence of the deposition rate and grain size on the F/Zn atomic ratio in the starting solution.

ties of the films. It was found that, undoped and fluorine doped zinc oxide thin films prepared at 425°C, show the highest electrical conductivity. In this work the effects of the fluorine incorporation on the optical and electrical properties are presented, for films deposited at that substrate temperature.

3.1. Film structure and composition

The X-ray diffraction spectra for fluorine doped ZnO thin films prepared at 425°C, shown in Fig. 1, indicate that the films are of polycrystalline nature. These films show a strong peak along [002] direction; therefore the crystallites are highly oriented with their *c*-axes perpendicular to the plane of the substrate. This result is in agreement with those reported for ZnO thin films prepared by the same and other

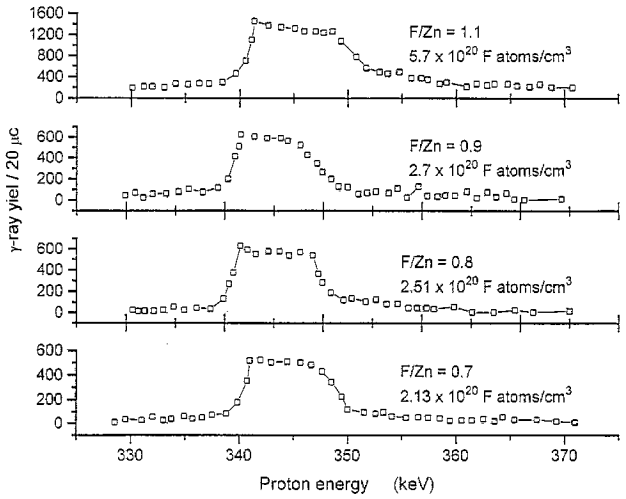

Fig. 3. Experimental excitation curves of the $^{19}F(p,\alpha\gamma)^{16}O$ reaction of fluorine in ZnO thin films prepared at different F/Zn atomic ratios in the starting solution. It shows the fluorine concentration in the films for each value of the F/Zn atomic ratio in the starting solution.

process [8,10,12,13,20]. On the other hand, from Fig. 1 an increase in F/Zn atomic ratio does not affect the preferential growth of the films, and hence the dopant level in the starting solution does not affect the lattice parameters of ZnO crystalline structure [36]. The crystal grain sizes were determined from the full width at half-maximum of the (002) X-ray peak using standard procedures. There is a fluorine incorporation in the films as long as the F/Zn atomic ratio increases in the starting solution, and its effect, is shown on the deposition rate and the grain size of the films. The behavior of the deposition rate and the grain size of the films as a function on the F/Zn atomic ratio are shown in Fig. 2. It can be seen that the deposition rate decreases when the F/Zn atomic ratio increases, whereas high dopant levels in the starting solution, prevent the grain growth in the [002] direction. The grain size follows the behavior shown in Fig. 2.

The reduction of deposition rate for films deposited at that substrate temperature can be explained if it is considered that the bond dissociation energy of H—F (136.2 kcal/mol) is bigger than those of F—Zn (88 kcal/mol) and O—Zn bonds (67.9 kcal/mol) [37], thus the formation of H—F molecules is more probable than the formation of F—Zn and O—Zn molecules. Then, if the concentration of NH_4F increases in the starting solution, the formation of HF is presented and a chemical etch could take place at the same time that deposition. On the other hand, the behavior of the grain size shown in Fig. 2 can be explained if it is considered that fluorine atoms do not substitute oxygen atoms, instead they are segregated at grain boundaries or at the film surface and hence, the number of the nucleation centers is reduced; or formation of ZnF_2 compound which is growing at the same time that ZnO:F films is probable [38]. Taking into consideration the preferential growth shown in Fig. 1, it can be concluded that fluorine incorporation in the ZnO thin films is taking place at oxygen sites in the ZnO lattice without effecting the lattice parameters and also, fluorine atoms are incorporated at the grain boundaries or at the film surface as its has been observed for other dopants [39]; meanwhile reduction in the crystal grain size could be due to the formation of ZnF_2 compound.

Fluorine has been identified as an impurity which improves the electrical properties of ZnO [15], but a large amount of F affect the crystalline structure. In consequence, it is important to determine its concentration as precisely as possible. The fluorine atomic concentration values reported here (see Fig. 3), obtained by RNR technique, are relative values to a target of LiF with a known amount of fluorine. With this target it was possible to assign a scale to the vertical axis of ZnO:F excitation curve in units of fluorine atoms per cubic centimeter: 220 γ-ray counts/20 μC (above the background) correspond to 10^{20} F atoms/cm^3 [34,35]. Fig. 3 shows the γ excitation curves obtained from four ZnO:F samples prepared at different F/Zn atomic ratios. No good signal-to-background ratio was obtained for samples prepared with F/Zn values lower than 0.7 due to the sensitivity of the technique. Fig. 3 shows that there is a

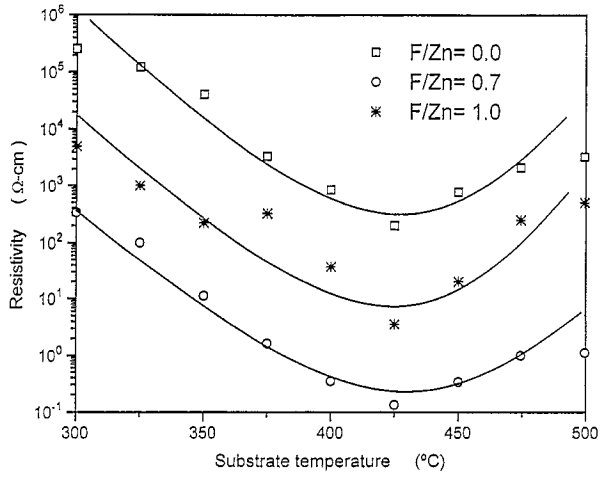

Fig. 4. Electrical resistivity for undoped and fluorine doped ZnO thin films.

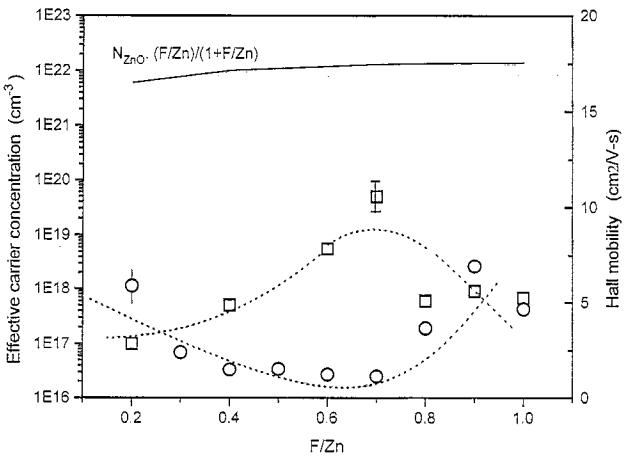

Fig. 6. Hall mobility (○) and effective carrier concentration (□)as a function of F/Zn atomic ratio in the starting solution.

rise in the signal near 340 keV, which correspond to the surface of the films. All the curves show a fluorine accumulation layer near the surface, and a reasonably flat concentration in the bulk of the film. In the high energy region, a fall-off appears that corresponds to the film-substrate interface, indicating that fluorine did not penetrate the substrate. It has been found that the fluorine concentration in these films is always smaller than that of the starting solution. This behavior is expected due to the high volatility of the fluorine compounds which are produced during the film deposition. The fluorine concentration on the ZnO:F thin films surface, that is evident from Fig. 3, are supporting our argument for the incorporation of fluorine atoms at film surface.

3.2. Electrical properties

Fig. 4 shows the evolution of the electrical resistivity (ρ) of the films with substrate temperature. The electrical resistivity for undoped and fluorine doped ZnO thin films reach a minimum for the same specific value of $T_s = 425$°C. But unlike other published works, we do not find any shift of the substrate temperature at which this minimum is reached as the doping level increases (as for SnO_2 [40], SnO_2:F [41] and ZnO:In [25]). Then, it is possible that the excess of cation species attributed to this phenomena are not present in our films, and hence, the reduction on ρ, shown in Fig. 4, is only attributed to fluorine atoms incorporated that are electrically active. The main effect that is expected by the dopant addition is a strong variation on ρ of the deposited films. This is shown in Fig. 5 as a function of the doping level at the starting solution. It should be noted first, that ρ falls as F/Zn increases, but after a critical value, the electrical resistivity goes up. This is an unexpected behavior for a fluorine-doping. The grain size reduction that we have observed in this doping range can explain this effect [42] as it will be described later.

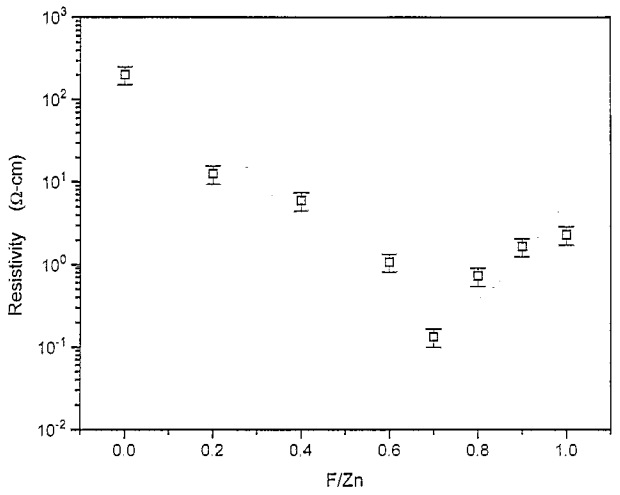

Fig. 5. Effect of F/Zn atomic ratio on the electrical resistivity of ZnO:F thin films prepared at $T_s = 425$°C.

Good transparent conductors with high values of fig.s of merit should have the highest possible carrier mobility (μ) [43]. Then, it is important to study the evolution of μ as a function of various deposition parameters. The electron mobility has been determined from the product of Hall coefficient and the electrical conductivity. Fig. 6 depicts the carrier mobility behavior of ZnO:F thin films as a function of the F/Zn atomic ratio. As we can see, μ values are not so high as required for having a good transparent conductor even if they are compared with lightly doped single crystal ZnO (typically value around 180 cm^2/V per s), but they are similar to those reported for polycrystalline ZnO undoped and doped with Al, In, F prepared by several processes [12,8,14,15]. These lower values may be expected for polycrystalline films because the carriers undergo scattering by the grain boundaries. In fact, this cannot be explained in an isolated way, because of its dependence on other factors, like the carrier concentration, the height of the potential barriers at the grain boundaries, etc. Then, in the following

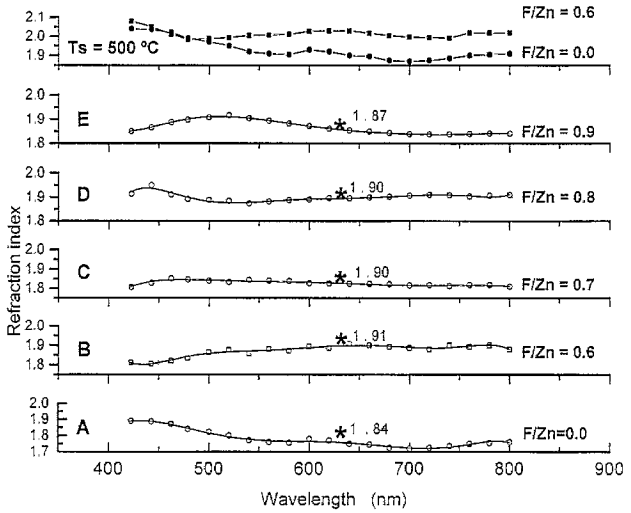

Fig. 7. Plots of refractive index as a function of wavelength for undoped and fluorine-doped ZnO thin films prepared at 425°C. The upper graph shows n vs. λ fo undoped and fluorine-doped ZnO thin films prepared at $T_s = 500$°C.

we are going to be concerned with these factors in order to find a reasonable explanation to this behavior.

As expected, the addition of fluorine atoms in the ZnO thin films may induce modifications on effective carrier concentrations (n) and their Hall mobility, as it is shown in Fig. 6. The carrier concentration tends to increase up to a value of 0.7 for the F/Zn atomic ratio, and from this, we observe a strong decrement while the carrier Hall mobility behaves inversely. That means that, the increase in fluorine concentration, increases the scattering and therefore, decrease the mobility, behaves like ZnO 'single crystal' [44]. The same behavior has been reported by Hu and Gordon [15] for ZnO:F prepared by atmospheric pressure CVD. The grain size follows a similar behavior as that of the carrier concentration as a function of the F/Zn atomic ratio while the carrier Hall mobility behaves inversely. As it is known, the extent of the 'flat' region of the bands between grain boundaries increases as the grain size does. Then, the height of the potential barriers at the grain boundaries could also be lowered by that way. This could explain the improvement on the average electrical transport properties through the film, even if the mobility carrier is decreased. Then, the dopant might start to incorporate more efficiently to the host lattice from a critical value (F/Zn≈0.4, see Fig. 6), modifying significantly the electrical and optical properties of the films. This seems to be supported by observing that the effective carrier concentration follows an inverse behavior to that shown by the electrical resistivity, as a function of the F/Zn atomic ratio. In this way, the increase in the carrier concentration with F/Zn atomic ratio, up to F/Zn ≈ 0.7, could be related to the incorporation of fluorine at substitution sites. The decrease observed in the effective carrier concentration and the increase in the electrical resistivity with the subsequent addition of fluorine to the starting solution, can be explained if: (a) fluorine atoms are located at interstitial sites instead of replacing anion sites giving rise to a large number of crystalline defects; and/or (b) a compound other than ZnO is growing at the same time that of ZnO:F, as it was already suggested [31].

On the other hand, as it was previously reported by Major et al. [20], in doped ZnO thin films the height of the potential barriers at the grain boundaries increases with the majority carrier concentration until a given value, then it decreases after a certain critical value is reached. This could explain the decreasing trend in the mobility as the carrier concentration increases up to F/Zn = 0.7. Similarly, a decrease in the height of the potential barrier gives rise to the increase of the mobility observed for F/Zn > 0.7 in the solution. Besides in this range, the conduction might be controlled by the presence of fluorine atoms at the grain boundaries [45]. Further studies are in progress to find an explanation for this behavior.

Similar results have already been reported for fluorine- and antimony-doped tin oxide [41,45,46] thin films, but not for doped ZnO ones. Straight line in the upper part of the graph corresponds to the carrier concentration that we could expect if each fluorine atom incorporates as an electrically active impurity, and acts as donor. We may also notice that, in the best case ($T_s = 425$°C, F/Zn ≫ 0.7), the effective carrier concentration, as measured by the Hall–Van der Pauw technique, is only a small fraction (in the order of the 1/400) of the fluorine concentration in the solution and an order of magnitude less that of the F incorporated at the films found by RNR technique (see Fig. 3). This could explain why the electrical results are so limited.

3.3. Optical properties

In order to know the effect of fluorine incorporation on the optical properties of ZnO:F thin films, we measured the optical transmittance and specular reflectance for undoped and fluorine doped ZnO thin films prepared at different substrate temperatures.

It was found that the optical transmittance of undoped ZnO thin films prepared at different substrate temperatures is improved as the substrate temperature increases due to an increases in the grain sizes [31]. Similar behavior was found for doped ZnO thin films at values of F/Zn ratio less than 0.5; but for F/Zn > 0.5, the mean transparency goes down due to the textured surface of the film and powdery nature of the deposited material. Due to the fact that for a F/Zn atomic ratio bigger that 0.5, the fluorine incorporation at ZnO thin films decreases the crystal grain sizes and inhibit the ZnO crystal growth as it was suggested by X-ray diffraction patterns, or it favors the formation of a new compound as has been suggested [31], we only analyzed the optical properties for ZnO:F thin films prepared with a F/Zn atomic ratio in these range.

Taking into account the electrical behavior of our films, it was chosen a substrate temperature of 425°C to study the

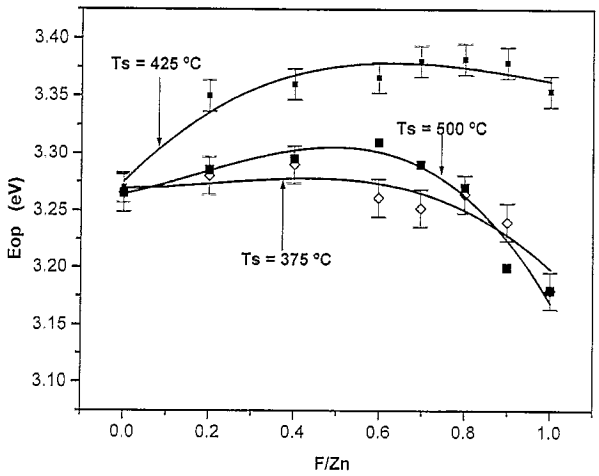

Fig. 8. Optical band gap as a function of F/Zn atomic ratio for different temperatures.

evolution of the wavelength dependence of refraction index (n) of the films with respect to F/Zn atomic ratio. The values of n for wavelengths between 0.5 and 0.9 μm (far away from the absorption edge), were calculated from the transmittance spectra and the method developed by Manifacier et al. [33] with a $\Delta n/n = 4\%$. Fig. 7 depicts the evolution of n in the visible region. From Fig. 7 it is clear that the fluorine incorporation at the films raises the refraction index value. Comparing the A and B graphs ($T_s = 425$°C) with the upper graphs ($T_s = 500$°C), it can see that n tends to get a value close to 2.0 and 1.9 for doped and undoped ZnO thin films, respectively, prepared at high substrate temperature; meanwhile n acquires values of less than 1.9, for lower substrate temperature. This behavior could be explained if we consider that the crystal grain sizes of ZnO:F are bigger at high substrate temperature, then they produce high optical transmission and an increase in the refraction index; while at low substrate temperature, the crystal grain sizes are smaller. On the other hand, for $T_s = 425$°C, it can observed that the F/Zn atomic ratio does not produce a strong effect in the n values of the films. Then it could be considered that, in the visible region, far away from the absorption edge, the refraction index is almost constant with a value of 1.9. This value is less than that reported for single-crystal ZnO and it could be attributed to the polycrystalline nature of our films.

The absorption coefficient α was determined from transmission and reflection measurements using the equation given by Chopra [47]. The optical band gap (E_g) of the undoped and fluorine doped ZnO thin films were deduced from the photon energy dependence of the absorption coefficient considering the material as a direct band gap semiconductor. Then using the square root energy dependence of α, E_g is determined by locating the intercept of α^2 vs. $h\nu$ plot on the $h\nu$ axis. Fig. 8 shows the effect of the F/Zn atomic ratio on the E_g values for three different substrate temperatures. It can see that the band gap first increases as the F/Zn atomic ratio increases. However, higher F/Zn atomic ratio decreases the E_g values; for the three substrates temperatures considered. This behavior could be attributed to the way that the fluorine atoms have been incorporated into the film. If F is located at substitution sites, then there is an increase in the carrier concentration, and consequently, the band gap widening shown in Fig. 8 could be due to the Moss–Burstein effect. This effect is taken place for F/Zn $\leq$ 0.7. On the other hand, the trend of decreasing E_g for F/Zn atomic ratio values bigger that 0.5, at that substrate temperature, could be attributed to the poor crystallinity of the prepared films or to the formation of the new compound based on F and Zn as has been proposed.

4. Conclusions

The electrical properties of ZnO thin films prepared by the spray pyrolysis process depend strongly on the substrate temperature and the fluorine incorporation at the films. In all the cases there is a substrate temperature for which the electrical resistivity has a minimum value. For undoped ZnO thin films this behavior could be due to a Zn excess at the thin films.

The fluorine incorporation at ZnO thin films reduces drastically the electrical resistivity up to four orders of magnitude compared with the undoped ZnO thin films. There is a critical doping value in the starting solution for which the electrical resistivity of the ZnO:F thin films has a minimum value, corresponding to the maximum crystal grain size value measured for these thin films.

After the critical doping level value the behavior of μ and n is associated with both: (i) variation in the height of the potential barriers in the grain boundaries and (ii) the way in which the fluorine atoms are incorporated. The results obtained by the RNR technique have shown that the fluorine incorporation in the films is always higher that the majority carrier concentration.

The improvement obtained in the optical transmittance at high substrate temperatures could be associated with the increase observed in the crystal grain size of the undoped and fluorine doped ZnO thin films.

The refraction index in all the visible region, far away from the absorption edge, is not strongly affected by an increase in the substrate temperature. For undoped ZnO thin films, at lower substrate temperature the refraction index has a value around 1.8 while at highs substrate temperatures, its value is approximately 1.9. On the other hand, the fluorine incorporation at ZnO thin films raises the value of the refraction index, tending to get a value of 1.9 at lower substrate temperature and a value of 2.0 for high substrate temperature, in the visible region.

The fluorine incorporation at ZnO thin films increases the optical band gap. The dependence of the optical band gap on the F/Zn atomic ratio for ZnO:F thin films prepared at $T_s = 425$°C occurred through its dependence on the carrier

concentration in the form of the Moss–Burstein effect of band gap widening. The band gap narrowing effect found for lower and higher substrate temperatures for F/Zn > 0.7, could be associated with a poor crystallinity or the formation of a new compound based on F and Zn.

Acknowledgements

The authors wish to acknowledge to Leticia Baños for the technical assistance in XRD measurements and Jose Campos for the electrical measurements.

References

[1] W. Hirschwald, et al., in: E. Kaldis (Ed.), Current Topics in Materials Science, Vol. 7, North Holland, Amsterdam, 1981, Chapter 3.
[2] O. Madelung (Ed.), Data in Science and Technology: Semiconductors, Other Than Group IV Elements and III-V Compounds, Springer–Verlag, New York, 1992.
[3] Y. Nakagawa, Appl. Phys. Lett. 31 (1977) 56.
[4] P.K. Tien, Appl. Opt. 10 (1971) 2395.
[5] H. Nato, S. Tsubakino, T. Kawi, M. Ikeda, S. Kitagawa, M. Habara, J. Mater. Sci. 29 (1994) 6529.
[6] X. Wang, W.P. Careg, S.S. Yee, Sens. Actuators B 28 (1995) 63.
[7] H. Watanabe, Jpn. J. Appl. Phys. 9 (1970) 418.
[8] H. Sato, T. Minami, Y. Tamura, S. Takata, T. Mouri, N. Ogawa, Thin Solid Films 246 (1994) 86.
[9] F.S. Mahmood, R.D. Gould, A.K. Hassan, H.M. Salih, Thin Slid Films 270 (1995) 376.
[10] K.B. Sundaram, A. Khan, Thin Solid Films 295 (1997) 87.
[11] T. Hata, T. Minamikawa, O. Morimoto, T. Hada, J. Cryst. Growth 47 (1979) 171.
[12] H. Sato, T. Minami, T. Miyata, S. Takata, M. Ishii, Thin Solid Films 246 (1994) 65.
[13] Y. Li, G.S. Tompa, J. Vac. Sci. Technol. A 15 (3) (1997) 1063.
[14] J. Nishino, T. Kawarada, S. Ohshio, H. Saitoh, K. Maruyama, K. Kamata, J. Mater. Sci. Lett. 16 (1997) 629.
[15] J. Hu, R.G. Gordon, Solar Cells 30 (1991) 437.
[16] Y. Takahashi, M. Kanamori, A. Kondoh, Jpn. J. Appl. Phys. 33 (1994) 6611.
[17] Y. Ohya, H. Saiki, Y. Takahashi, J. Mater. Sci. 29 (1994) 4099.
[18] M. Izaki, T. Omi, Appl. Phys. Lett. 68 (17) (1996) 2439.
[19] D.E. Brodie, R. Singh, J.H. Morgan, J.D. Leslie, L.J. Moore, A.E. Dixon, Proc. 14th. IEEE Photovoltaic Specialists Conf., San Diego, CA, IEEE, New york p. (1980) 468.
[20] S. Major, A. Banerjee, K.L. Chopra, Thin Solid Films 108 (1983) 333.
[21] S. Major, A. Banerjee, K.L. Chopra, Thin Solid Films 125 (1985) 179.
[22] S.E. Demian, J. Mater. Sci. Mater. Electron. 5 (1994) 360.
[23] C. Messaoudi, D. Sayah, M. Abd-Lefdil, Phys. Stat. Sol. (a) 151 (1995) 93.
[24] M. Krunks, E. Mellikov, Thin Solid Films 270 (1995) 33.
[25] A. Tiburcio-Silver, J.C. Joubert, M. Labeau, J. Phys. III 2 (1992) 1287.
[26] T. Young Ma, S. Hyum Kim, H. Yul Moon, et al., Jpn. J. Appl. Phys. 35 (1996) 6208.
[27] C. Kun Ryu, K. Kim, Appl. Phys. Lett. 67 (22) (1995) 3337.
[28] G. Newman, Phys. Status Solidi (b) 105 (1981) 605.
[29] G. Heiland, Z. Phys. 148 (1957) 15.
[30] R.G.Gordon, Proc. Photovoltaics Prog. Rev., CP394 NREL/SNL, 1997, p. 39.
[31] A. Sanchez-Juarez, A. Tiburcio-Silver, A. Ortíz, Solar Energy Mater. Solar Cells 52 (1998) 301.
[32] S. Major, A. Banerjee, K.L. Chopra, K.C. Nagpal, Thin Solid Films 143 (1986) 19.
[33] J.C. Manifacier, J. Gasiot, J.P. Fillard, J. Phys. E 9 (1976) 1002.
[34] E.P. Zironi, J. Rickards, A. Maldonado, R. Asomoza, Nucl. Instrum. Methods B 45 (1990) 115.
[35] R. Asomoza, A. Maldonado, J. Rickards, E.P. Zironi, M.H. Farias, L. Cota-Araiza, G. Soto, Thin Solid Films 203 (1991) 195.
[36] D.J. Goyal, C. Agashe, M.G. Takwale, B.R. Marathe, V.G. Bhide, J. Mater. Sci. 27 (1992) 4705.
[37] R.C. Weast (Ed.), Handbook of Chemistry and Physics, 67th Edition 1986–1987, CRC Press, Boca Raton, FL.
[38] J. Elizalde-Torres, E.P. Zironi, G. Torres-Villaseñor, L.S. Cota, L. Baños, J. Rickards, S.M. Saniger, Mater. Lett. 26 (1996) 41.
[39] A. Tiburcio-Silver, J.C. Joubert, M. Labeau, Thin Solid Films 197 (1991) 195.
[40] J.C. Manifacier, M. De Murcia, J.P. Fillard, E. Vicario, Thin Solid Films 41 (1977) 127.
[41] A. Tiburcio-Silver, A. Maldonado, A. Escobosa, E. Saucedo, J.M. Montoya, J.A. Moreno, Appl. Surf. Sci. 70/71 (1993) 746.
[42] J. Orton, M.J. Powel, Rep. Prog. Phys. 43 (1960) 1265.
[43] G. Frank, F. Kauer, H. Köstlin, Thin Solid Films 77 (1981) 107.
[44] G. Heiland, E. Mollwo, F. Stöckmann, Solid State Phys. 8 (1959) 191.
[45] E. Shanti, A. Banerjee, K.L. Chopra, Thin Solid Films 88 (1982) 93.
[46] G. Frank, F. Kauer, H. K, H. östlin, F.J. Schmitte, Solar Energy Mater. 8 (1983) 387.
[47] K.L. Chopra, S.R. Das, Thin Film Solar Cells, Plenum Press, New York, 1983.